Journal of Materials Chemistry C

ROYAL SOCIETY OF CHEMISTRY

PAPER

View Article Online
View Journal | View Issue

Cite this: J. Mater. Chem. C, 2024, 12, 9999

Tetraphenylpyrazine-based chiral deep-blue dyes with high brightness for energy delivery†

Xiang He,‡[a] Canze Zheng,‡[a] Xin Deng,[a] Yingjuan Hong,[a] Miao Meng,[a] Chunxuan Qi,[b] Hai-Tao Feng,[b] Ming Chen*[a] and Ben Zhong Tang[c]

Received 4th April 2024,
Accepted 29th May 2024

DOI: 10.1039/d4tc01374c

rsc.li/materials-c

The search for deep-blue dyes with high luminescence efficiency in the aggregate state and high brightness is particularly important in optoelectronic application. Herein, based on a typical aggregation-induced emission (AIE) unit of tetraphenylpyrazine (TPP), four dyes were prepared by connecting it with chiral binaphthyl units *via* an acetylenic bond. The use of the TPP unit is critical to aggregation-enhanced emission (AEE) and deep-blue emission, whereas the merging of the binaphthyl unit is beneficial for molecular conjugation to remarkably improve absorption, photoluminescence (PL) quantum efficiency and brightness. Besides, the binaphthyl unit can serve as an axially chiral source to endow the deep-blue dyes with chirality. It was revealed that attaching a longer alkoxy chain to the dyes facilitates the formation of helical self-assemblies determined by chiral transfer but leads to an aggregation-caused emission (ACQ) effect. Moreover, using these deep-blue dyes as energy donors for energy delivery, other emissions and pure white light emission can be generated effectively *via* an energy transfer process based on a rational mixture of donors and acceptors in PMMA films. The device fabricated by coating this film onto a blue LED also emitted distinct and stable white light. This work provides a flexible way to design high-performance blue materials for potential applications.

Introduction

Organic emitters have attracted tremendous attention in various applications such as optoelectronic devices, fluorescent probes and smart materials for their good processability, flexible molecular design and low toxicity.[1] However, most of the organic luminogens such as pyrene, naphthalene and perylene bisimide are conjugated molecules with a planar conformation. They are prone to form π–π stacking upon aggregation to quench emission, which affects their practical application.[2] The emergence of aggregation-induced emission (AIE) or aggregation-enhanced emission (AEE) molecules will help resolve the aggregation-caused quenching (ACQ) effect found in traditional dyes.[3] The intrinsic property of AIE or AEE dyes is their twisted and flexible molecular conformation, which enables them to relax in the excited state in solution to annihilate or weaken the emission, while the conformational changes can be supressed to turn-on or enhance the emission by aggregation.[4] On this basis, many AIE and AEE dyes have been developed to show extremely high photoluminescence (PL) quantum efficiencies in the aggregate state, which is much desirable to meet diversified applications.[5] However, conformational torsion will exert some negative effect on their photo-

[a] College of Chemistry and Materials Science, Jinan University, Guangzhou 510632, China. E-mail: chenming@jnu.edu.cn
[b] AIE Research Center, Shaanxi Key Laboratory of Photochemistry, College of Chemistry and Chemical Engineering, Baoji University of Arts and Sciences, Baoji 721013, China
[c] School of Science and Engineering, Shenzhen Institute of Aggregate Science and Technology, The Chinese University of Hong Kong, Shenzhen (CUHK-SZ), Guangdong, China

† Electronic supplementary information (ESI) available. See DOI: https://doi.org/10.1039/d4tc01374c

‡ These authors contributed equally to this work.

Ming Chen

Ming Chen received his PhD from Zhejiang University in 2015 under the supervision of Prof. Ben Zhong Tang and Prof. Anjun Qin. Later, he conducted a postdoctoral research at Tang group at HKUST from 2015 to 2018. In June 2018, he joined Jinan University as an associate professor. His research focuses on the development of functional dyes for imaging and therapeutic applications based on pyrazine building blocks through multiple approaches (including small-molecule engineering, supramolecular chemistry and polymerization strategy).

physical behaviour. In particular, the π electronic cloud overlapping between the inner units is weakened to decrease molecular conjugation, which is unfavourable for absorption.[6] It suggests that a good light-harvesting ability is another key factor to determine their applications.[7] Thus, designing high-brightness AIE or AEE dyes by a combination of high PL quantum efficiencies and strong absorptions is challenging.

Furthermore, despite their potential to exhibit AIE or AEE effects based on their structural design, many fluorescent dyes eventually show a quenched fluorescence emission behaviour in the aggregate state.[8] For example, Tang reported two diphenyldibenzofulvene-based dyes, which exhibited strong emissions in the crystal state but almost quenched emissions due to unformed aggregation.[9] This indicates that the aggregation-state structure has a profound effect on emission behaviour. However, it is still a challenge to artificially control the aggregate-state behaviour to deeply understand this relationship. Recently, some studies have revealed that for designing high-efficiency photothermal conversion agents, attaching long alkyl chains to the dyes can space the molecules in the aggregate state while vigorous intramolecular motions can take place after excitation due to less steric restriction to boost the non-radiative energy dissipation.[10] Thus, it is particularly interesting to use such a strategy to investigate the effect of side chain length on the aggregate-state behaviour of dyes as well as their emission properties, which is instructive to design the luminescent materials with desirable functions and applications.

The search for high-performance blue materials is always important in the optoelectronic field, as they can not only realize one of the three primary colours but also act as hosts to excite other emissions.[11] However, the drawbacks of low luminescence efficiency and bad light purity still hamper their applications. Tetraphenylpyrazine (TPP) belongs to a class of heterocycle-based AIE cores, which shows the merits of facile synthesis, good stability, tunable electronic property, rich nitrogen site, *etc.*[12] Many works have demonstrated the superiority of TPP in designing functional materials. For example, the AIE molecules with large two-photon absorption cross sections can be realized by using TPP as an acceptor to induce intramolecular charge transfer.[13] A metal–organic framework with TPP as the ligand can fluorescently recognize arginine due to the specific hydrogen bond interaction between the guanidine group in arginine and the nitrogen atom in TPP.[14] It is also reported that TPP is favourable to boost the intersystem crossing to enhance the photosensitization by supressing the internal conversion caused by the intramolecular motions in a photosensitizer design.[15] The use of TPP in developing blue materials is also promising. By decorating TPP with phenanthroimidazole-based group, an AIE emitter with sky blue emission can be generated with its fabricated light-emitting device showing a high external quantum yield of 4.85%.[16] Moreover, TPP can be used to fabricate a blue-emissive amphiphilic organic cage to capture diketopyrrolopyrrole *via* a host–guest interaction, while their combined roles can contribute to a white light emission.[17] Much recently, we fabricated microfibers with a TPP-based AIE dye, which show a high PL quantum efficiency, narrow deep-blue emissions and good photo-stability. The fibers show a good waveguide effect with a low optical loss coefficient and can light up the other emissions in the microscale.[18] Although much efforts have been devoted to design blue materials based on such a building block, achieving blue AIE or AEE dyes with high brightness is still desirable.

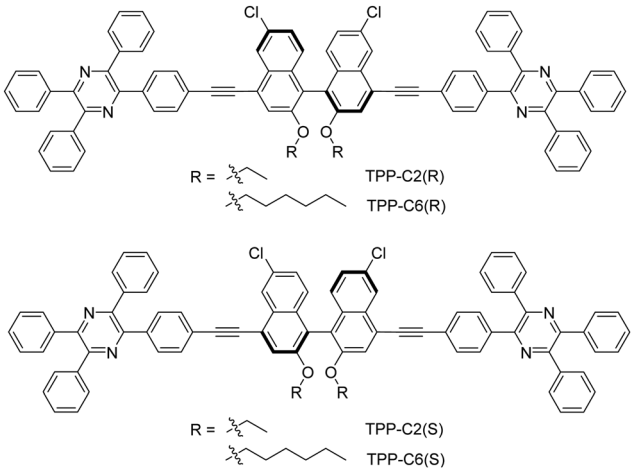

Chart 1 Molecular structures of TPP-C2(R), TPP-C2(S), TPP-C6(R) and TPP-C6(S).

In this work, based on a typical AIE unit of TPP, we prepared four dyes (two pairs of chiral enantiomers) named TPP-C2(R), TPP-C2(S), TPP-C6(R) and TPP-C6(S) by connecting chiral binaphthyl units with an acetylenic linker (Chart 1). The utilization of the TPP unit is crucial to the AEE effect and deep-blue emission due to its intrinsic property. The merging of binaphthyl units can obviously increase the molecular conjugation to determine a high light absorption ability $>8 \times 10^4$ cm^{-1} L mol^{-1}, a PL quantum efficiency of ~72% and brightness $>5.5 \times 10^4$ cm^{-1} L mol^{-1}, which was particularly desirable in the practical applications. Moreover, derived from the binaphthyl units, the molecular chirality was successfully achieved *via* chiral transfer, as observed from the CD spectra. The molecular chirality can transfer to their self-assembled aggregates. In particular, in TPP-C6(R) and TPP-C6(S) with a longer alkoxy chain, the self-assembled fibers with an opposite helix can be formed, which can be observed using a scanning electron microscope (SEM) and a fluorescence microscope. However, we found that increasing the length of side groups can transform the AEE effect to the ACQ effect, suggesting that the emission behaviour is closely related to the aggregate-state structure affected by this factor. These dyes were further used as energy donors to excite the other emissions. We demonstrate that based on a rational mixture of these deep-blue dyes with other fluorescent dyes (Dye-G, Dye-O and Dye-R) in PMMA, the distinct green, orange and red emissions can be obtained, respectively, with an energy transfer efficiency close to 100%. The PL quantum efficiencies of these emissions were much better than their unity without a donor, indicating a superiority of utilizing them for energy delivery and magnifying emission. Moreover, by using these dyes as donors, the pure white light with a Commission International de L'Eclairage (CIE) coordinate of (0.33, 0.33) and a PL

quantum efficiency approaching 100% can generate through a controlled energy transfer effect. After coating the film onto the blue LED, the resulting device can give distinct and stable white light emissions. Thus, this work provides a strategy to design chiral dyes with deep-blue emissions and high brightness for potential optoelectronic applications.

Results and discussion

We designed four fluorescent dyes named TPP-C2(R), TPP-C2(S), TPP-C6(R) and TPP-C6(S) by linking the TPP unit and the chiral binaphthyl unit through a Sonogashira coupling reaction, while the length of the alkoxy chain appending to the binaphthyl unit is tunable (Chart 1). Our design principle is as follows: (1) the incorporation of AIE-active TPP unit would endow the molecules with blue emissions and high luminescence efficiencies, while the binaphthyl unit connected by the acetylene bond would remarkably enhance the molecular conjugation to improve the absorptivity, which collectively render them ideal luminescent materials; (2) the binaphthyl unit can not only be used as a conjugation group but also act as an axially chiral source to endow the resulting blue dyes with chirality; (3) the different lengths of alkoxy chain would make the aggregate-state behaviour of dyes adjustable to affect their luminescence and self-assembly properties. The synthetic routes of these dyes are shown in ESI.† After successive reactions, the products were obtained *via* purification by column chromatography with their structures well characterized by ^{1}H and ^{13}C NMR and high-resolution mass spectroscopies (Fig. S1–S12, ESI†). The thermal stability of these molecules was investigated by thermogravimetric analysis (TGA) at a heating rate of 10 °C under nitrogen. The results indicated that the temperatures at their 5% weight loss were all ~390 °C, indicating good stability resistant to thermal decomposition irrespective of the alkoxy chain length (Fig. S13, ESI†).

The UV-Vis spectra indicated that these dyes almost possessed an identical absorption profile in THF (Fig. 1A). The long-wavelength absorption at 383 nm was ascribed to the extended conjugation by the molecular design, while the short-wavelength absorption at 344 nm was determined by the local excitation such as the TPP unit in the molecules. Moreover, their molar absorptivity (ε) has increased to more than 8×10^4 cm^{-1} L mol^{-1} when compared to TPP (2.4×10^4 cm^{-1} L mol^{-1}) (Table S1, ESI†).[12a] This suggested that the combination of TPP with the binaphthyl unit has remarkably improved the light-harvesting ability. Moreover, in comparison to the solutions, a red-shift effect by ~12 and ~18 nm was found in the powders and doped PMMA films, respectively, which was probably due to the increased intermolecular interaction caused by the aggregation or changed molecular

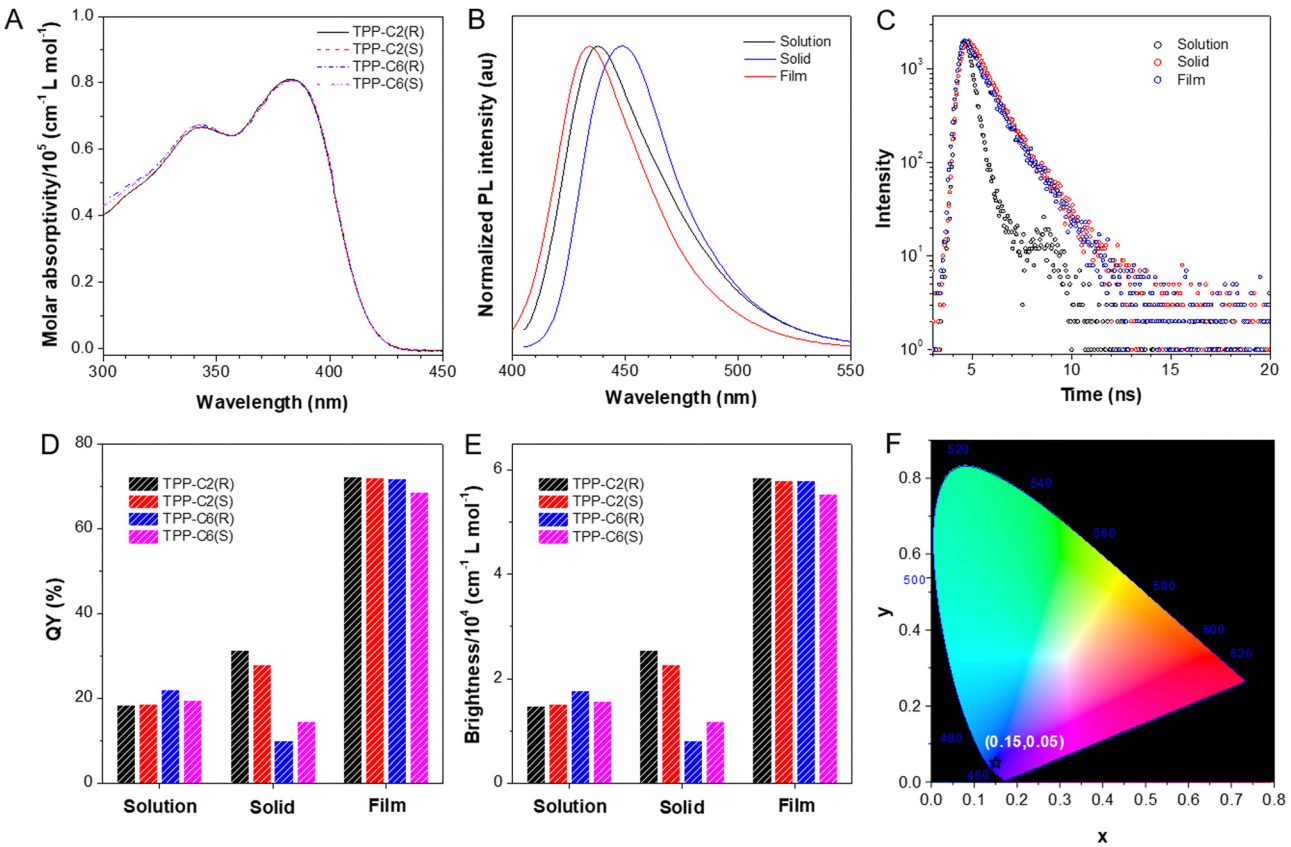

Fig. 1 (A) UV-Vis spectra of dyes in THF (10 μM). PL (B) spectra and (C) decay curves of TPP-C2(R) in solutions, powders and PMMA films. (D) Quantum yield (QY) and (E) brightness of dyes in solutions, powders and PMMA films. (F) CIE coordinate of dyes in PMMA films.

conformations affected by the external environment (Fig. S14, ESI†). The PL spectra showed that they all have an emission maximum at 438 nm in the solutions, while a slight red-shift effect by ~12 nm can be found in their powders (Fig. 1B and S15, ESI†). This is in accordance with the UV-Vis spectral results that the intermolecular interaction increased to some extent due to the aggregate effect. However, the emission of PMMA films was a bit bluer than that of the solutions. This is because their structural relaxation after excitation has been remarkably reduced by the rigid media, which affected the molecular levels.[19] These dyes possessed short-lived fluorescence emissions as recorded by the transient PL spectra (Fig. 1C and S16, ESI†). Moreover, their PL quantum yield (Φ_F) in the solutions, powders and films was evaluated by an integrating sphere. The results indicated that the Φ_F values of TPP-C2(R) and TPP-C2(S) in the solutions were 18.3% and 18.7%, respectively, which were much smaller than that in the powders (31.3% and 28.0%) (Fig. 1D and Table S1, ESI†). Thus, the AEE effect was realized in TPP-C2(R) and TPP-C2(S), which was attributed to the introduction of the TPP unit. Because TPP is AIE-active, it may endow the resulting molecules with a high conformational freedom, which will provide structural relaxation in the excited state in the solution to weaken the emission, while such relaxation can be restricted in the aggregate state to enhance the emission.[12a] However, the emission of the dyes can be tuned by the aggregate-state behaviour affected by the appended alkoxy chains. For example, TPP-C6(R) and TPP-C6(S) possessed similar Φ_F values to TPP-C2(R) and TPP-C2(S) in the solutions. However, their Φ_F values dropped to 10.0% and 14.6%, respectively in the powders. Thus, increasing the length of side groups makes them suffer from the ACQ effect. This was because the much longer alkoxy chains in TPP-C6(R) and TPP-C6(S) may provide much flexible surroundings while the excited-state intramolecular motions were still easy to take place to boost the non-radiative transition. The Φ_F values of all dyes were recorded as high as ~72% in the films. This confirmed that a rigid environment can be formed by PMMA to prohibit the intramolecular motions to further boost the emissions.[19] Normally, the brightness ($\varepsilon\Phi_F$) is an important parameter to evaluate the luminescent materials by a combinative consideration of their absorption and emission properties. Here, the brightness of these dyes in these films was calculated to be more than 5.5×10^4 cm^{-1} L mol^{-1}, which were superior to the most reported conventional dyes and AIE dyes (Fig. 1E and Table S1, ESI†).[20] Moreover, the Commission International de L'Eclairage (CIE) coordinates of these films were (0.15, 0.05) (Fig. 1F and Table S1, ESI†). All these suggested that these dyes are deep-blue materials with excellent brightness, which were particularly desirable in the practical applications.

Moreover, to provide more insights into the photophysical properties of these dyes, their excited-state decay rates were evaluated using the formula of $k_r = \Phi_F/\tau$ and $k_{nr} = (1 - \Phi_F)/\tau$, where k_r, k_{nr} and τ are the radiative and non-radiative decay rates, and excited-state lifetime, respectively. Their calculated k_r values in the solutions were $\sim 0.36 \times 10^9$ S^{-1}, which were much larger than that in the powder ($0.12–0.28 \times 10^9$ S^{-1}) (Table S2, ESI†). It was corresponding to the possible formation of excimers caused by the binaphthyl unit in the aggregate state, which impaired the radiative transition process. Moreover, the k_{nr} values of these dyes in the solutions were $1.15–1.67 \times 10^9$ S^{-1}. However, in the powders, the k_{nr} values of TPP-C2(R) and TPP-C2(S) reduced remarkably as the excited-state intramolecular motions were prohibited by the aggregation. The much obvious reduction in k_{nr} than k_r from the aggregate to solution state can lead to the AEE effect. By comparison, the k_{nr} values of TPP-C6(R) and TPP-C6(S) were nearly as twice as that of TPP-C2(R) and TPP-C2(S) and close to that of their solutions. This suggested that the introduction of long alkoxy chains into the molecules can facilitate the intramolecular motions to quench the emission even when they were in the aggregate state. Besides, a much larger k_r value of $\sim 0.61 \times 10^9$ S^{-1} can be found in their films in comparison to the solutions and powders. This may be due to two factors: (1) in PMMA films, the molecular conjugation may increase due to the conformational change and (2) the molecules were diluted by the films, while the formation of excimers may be effectively prohibited. Furthermore, the PMMA matrix also played a positive role in supressing the non-radiative transition as reflected by their much reduced k_{nr} value of $\sim 0.25 \times 10^9$ S^{-1}, suggesting that this rigid matrix was pretty evident to restrict the intramolecular motions in the excited state.

In this work, we employed the binaphthyl unit not only because of the role in strengthening the molecular conjugation but also in consideration of a chiral source to bestow the dyes with chirality. To check this, their circular dichroism (CD) spectroscopies in the solutions were investigated. As shown in Fig. 2A, the CD spectra of TPP-C2(R) and TPP-C2(S) in the solutions showed distinct Cotton effects and a mirror-image relationship at a wavelength in the range from 230 to 450 nm. The CD signals at ~260 nm were attributed to the binaphthyl moiety, whereas the CD bands centered at ~390 nm and 350 nm were mainly decided by the whole molecule and TPP unit, respectively, which were corresponding to the absorption peaks in the UV-Vis spectra. This indicated that the chirality of the binaphthyl unit has successfully transferred from the part to the whole, and two chiral enantiomers with deep-blue emissions and AEE property were obtained. Besides, a very similar phenomenon was observed in the CD spectra of TPP-C6(R) and TPP-C6(S) though they experienced an ACQ effect (Fig. 2B).

Many studies indicated that the molecular chirality may aid in the self-assembly to definite morphologies such as vesicles, spheres and fibers.[21] Would such self-assembly behaviour be achieved by our dyes? To answer this question, we prepared the samples with TPP-C2(R) and TPP-C2(S) dissolved in a $CHCl_3$/CH_3CN (v/v = 1 : 1) mixture. Because $CHCl_3$ and CH_3CN separately served as good and poor solvents, this moderate mixture may induce the formation of self-assemblies with the time. However, there was nothing detectable in the solutions by naked eyes during a continuous 5-day observation. On day 5, the sample was extracted and casted onto the silica plate, followed by studying using a scanning electron microscope (SEM). The results indicated that there were almost no definite self-assemblies, which can be observed in the image, suggestive

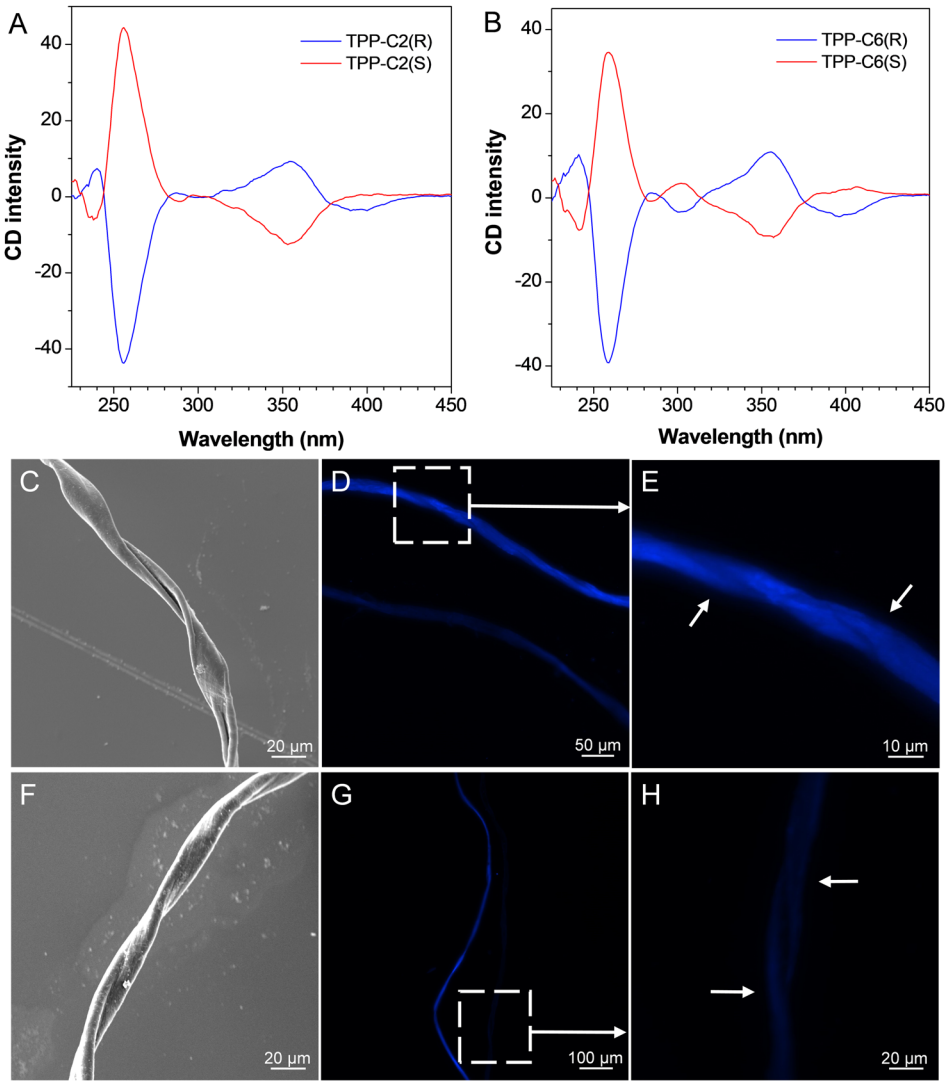

Fig. 2 CD spectra of (A) TPP-C2(R) and TPP-C2(S) and (B) TPP-C6(R) and TPP-C6(S) in THF. SEM and fluorescence images of self-assemblies formed by (C)–(E) TPP-C6(R) and (F)–(H) TPP-C6(S) in a $CHCl_3/CH_3CN$ (v/v = 1 : 1) mixture.

of a worse self-assembly behaviour (Fig. S17, ESI†). In sharp contrast, a much clear structure can be formed when TPP-C6(R) and TPP-C6(S) were dissolved in the same mixture. For TPP-C6(R), the explicit fibers with a diameter of ~15 μm can be found by SEM, which were uniformly right-handed (Fig. 2C). A similar phenomenon can be observed using a fluorescence microscope under UV light excitation, while the deep-blue fibers with a specific helix can be discerned (Fig. 2D and E). Moreover, although the fibers of similar sizes can be generated by TPP-C6(S) under the same condition, they were almost left-handed, which were confirmed by both SEM and fluorescence microscopy (Fig. 2F–H). This suggested that the molecular chirality has transferred to their self-assembled aggregates through a hierarchical approach, which ensured an efficient outcome for the generation of highly functional self-assembled structures.[22] In other words, the length of alkoxy chains appended to the chiral molecules played a vital role in this transfer behaviour.

The S_0 geometries of these dyes were optimized by B3LYP/6-31G(d,p), Grimme's DFT-D3.[23] The results indicated that these conformations were highly twisted, particularly in the TPP and binaphthyl moieties (Fig. S18, ESI†). Thus, the incorporation of the TPP unit may weaken the π–π stacking effect while restricting the intramolecular motions in the aggregate state to facilitate the emission. The twist between two naphthyl rings in the binaphthyl unit in the enantiomers was opposite with a dihedral angle larger than 70°. The remarkable conformational difference may ensure the chiral property of dyes due to the mirror symmetry. The electronic structure analysis suggested that the highest occupied molecular orbitals (HOMOs) of these dyes were mainly distributed on the central binaphthyl units, part of the peripheral TPP unit and the connected acetylenic bonds (Fig. 3). In contrast, more electronic clouds were found in the pyrazine rings of TPP besides the above-mentioned regions in their lowest unoccupied molecular orbitals (LUMOs). The successive electronic cloud distribution on the whole

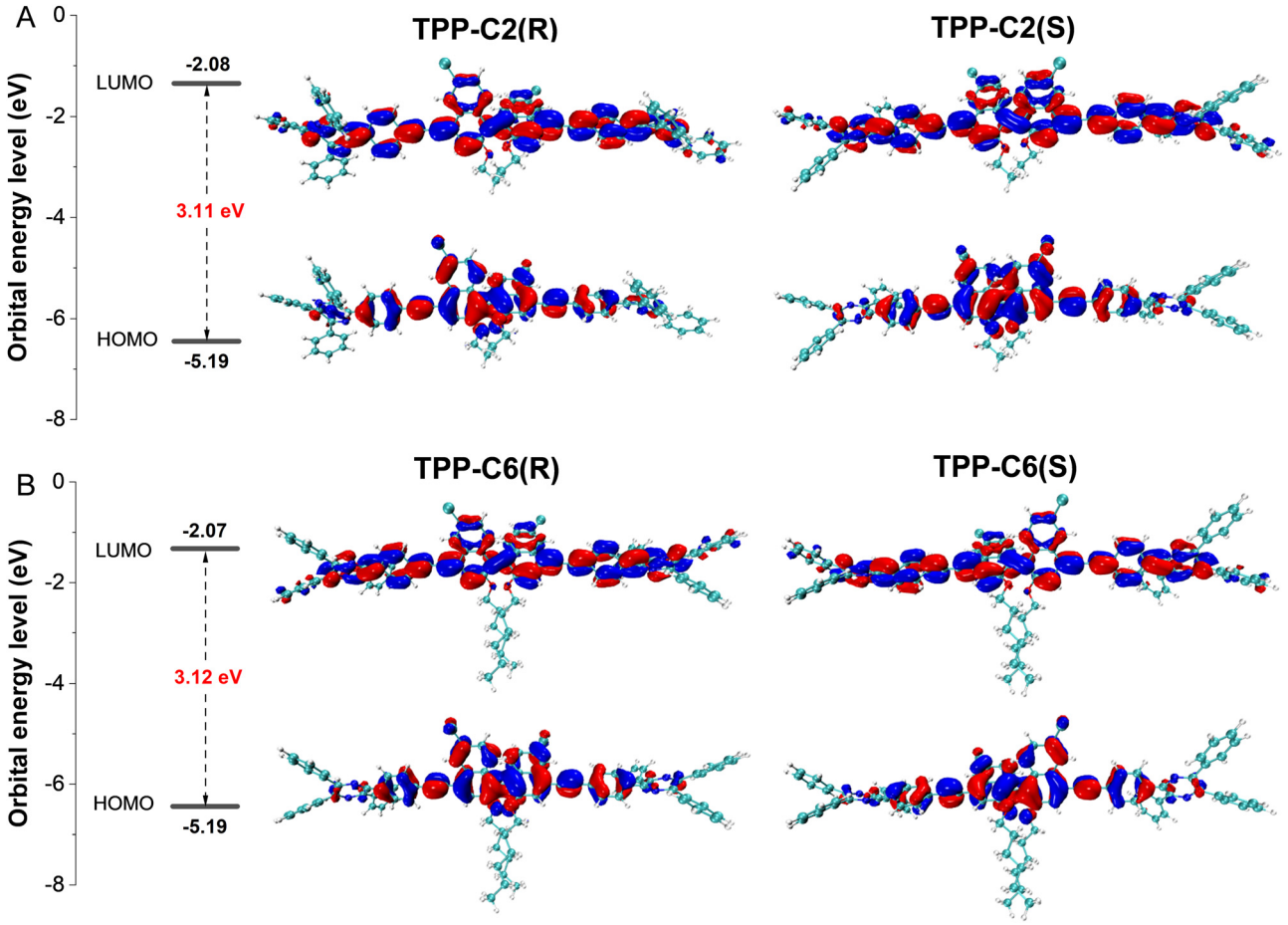

Fig. 3 Orbital distribution on S_0 conformations of (A) TPP-C2(R) and TPP-C2(S), and (B) TPP-C6(R) and TPP-C6(S) optimized by B3LYP/6-31G(d,p), Grimme's DFT-D3 and their energy levels.

molecules suggested that a good conjugation effect has been realized due to a good planarity between the naphthyl rings and the phenyl rings connected by the acetylenic bonds. Moreover, good electronic cloud overlapping between the HOMOs and LUMOs manifested that local state excitation is dominant in the excitation behaviour. Both factors can contribute to a high molar absorptivity and luminescence efficiency of the dyes. Moreover, we found that the molecular conformation as well as the electronic structure were less affected by the length of alkoxy chains, suggesting that such role exerted a negligible effect on their photo-physical properties at a molecular level.

With the high-brightness deep-blue dyes in the hand, we expected to utilize them as an energy host to excite the other emissions. In this work, three fluorescent dyes named Dye-G, Dye-O and Dye-R were adopted, with their structures shown in Fig. 4A. Most of these dyes have been proved to show the AIE effect with green, orange and red emissions, respectively, and possess a high luminescence efficiency.[24] We thus synthesized them according to the procedure reported in the literature with their structures well characterized by NMR spectroscopy (see ESI†). The PL study indicated that they showed emission maximums at 488, 578 and 614 nm in the films, while their absorption maximums were located at 401, 460 and 494 nm in THF, respectively (Fig. 4B and S19, ESI†). Note that the absorptions of these dyes have good overlapping with the emission of deep-blue dyes, indicating a theoretical possibility for the energy transfer from the donors to the acceptors. Indeed, when they are doped into deep-blue dyes with PMMA as a matrix, their emissions can originate remarkably with the increase in doping concentration accompanied by the decrease in blue light intensities. Moreover, the energy transfer efficiency was calculated using the formula of $\eta = 1 - (I_{DA}/I_D)$, where I_D is the emission intensity of donor initially, and I_{DA} is the emission intensity of donor after doping with the acceptor.[25] Our studies revealed that with a suitable mixing ratio, almost all the energies can be transferred from the donors to the acceptors after excitation (Fig. 4C and Fig. S20, ESI†). For example, when the ratio of TPP-C2(R) between Dye-G, Dye-O and Dye-R reached 2 wt% : 1 wt%, 7.3 wt% : 0.9 wt%, and 16.5 wt% : 0.8 wt%, very high η of 93.5%, 99.9% and 97.9% can be realized, respectively (Table S3, ESI†). Because TPP-C2(S), TPP-C6(R) and TPP-C6(S) behaved similarly in the PMMA films, they all possessed a similar energy transfer process with these dopants. Moreover, the average PL quantum efficiencies of these acceptors were recorded as high as 67.1%, 99.1% and 54.8%, respectively, which were much better than their pure state, suggesting that

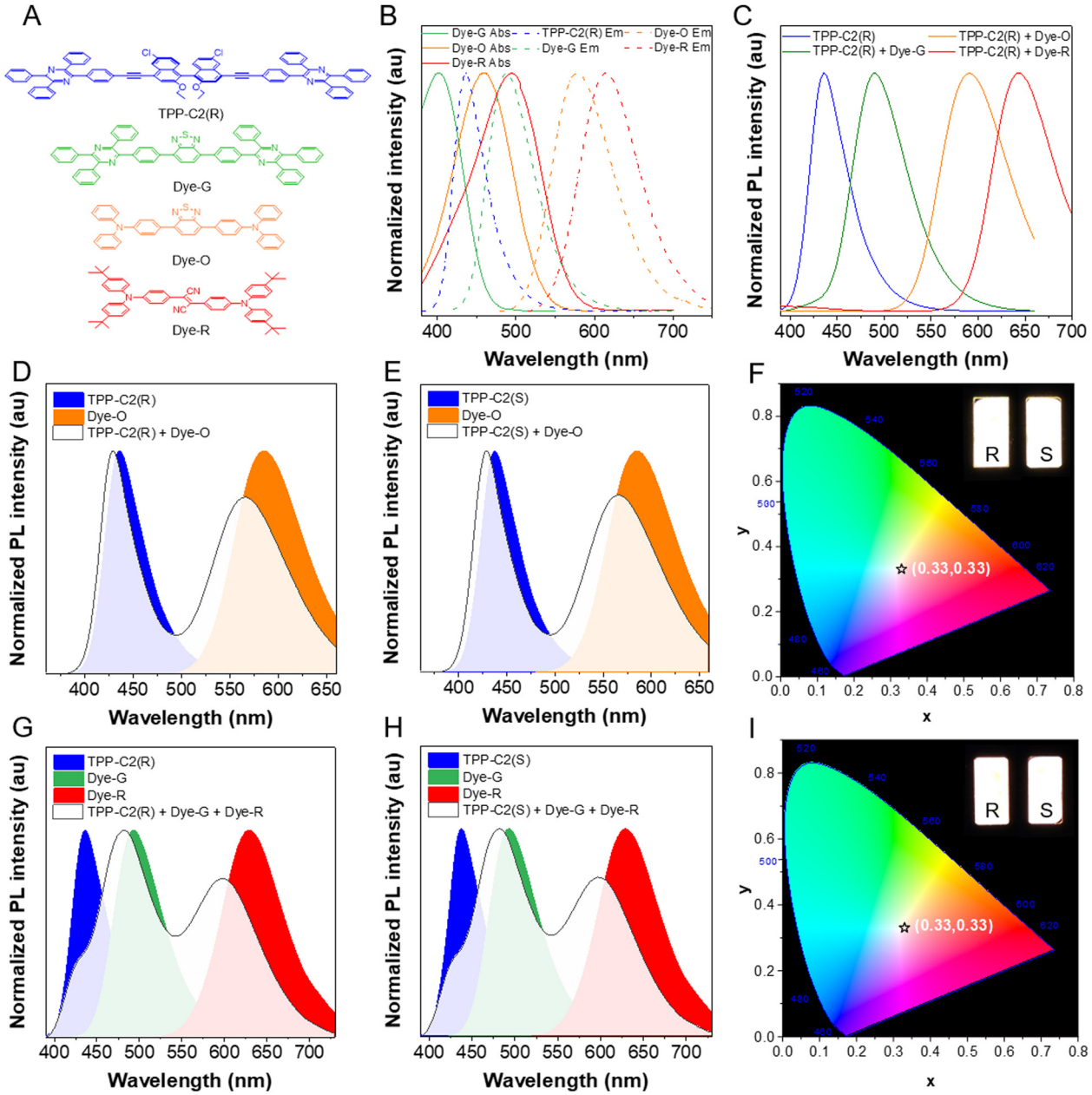

Fig. 4 (A) Molecular structures of TPP-C2(R), Dye-G, Dye-O and Dye-R. (B) UV-Vis or PL spectra of these dyes. (C) PL spectra of TPP-C2(R) and Dye-G, Dye-O and Dye-R after energy transfer. PL spectra of (D) TPP-C2(R) and (E) TPP-C2(S), Dye-O and their generated white light after mixing. (F) CIE coordinate of white light in D and E. PL spectra of (G) TPP-C2(R) and (H) TPP-C2(S), Dye-G, Dye-R and their generated white light after mixing. (I) CIE coordinate of white light in (G) and (H). Inset: photographs of white light films under 365 nm UV light.

it was attractive to magnify the emissions of other dyes through an energy transfer approach with our deep-blue dyes as energy donors (Table S3, ESI†).[26]

White light plays an essential role in the illumination in our daily life.[27] The white light is always realized by a partial energy transfer from the blue host to the other guest, while a mixed blue emission and other emissions can generate a consecutive spectrum similar to the visible light region in the sunlight.[28] In this regard, TPP-C2(R) or TPP-C2(S) was taken as a host to excite Dye-O. While the ratio of TPP-C2(R)/TPP-C2(S) : Dye-O were all 1 wt% : 0.3 wt%, the distinct white light emissions comprising the blue light from the donor and the orange light from the acceptor can emerge with their PL quantum efficiencies approaching 100% (Fig. 4D and E and Table S3, ESI†). The white emission can also be obtained by a controllable mixture of TPP-C2(R) or TPP-C2(S) with Dye-G and Dye-R in PMMA if the emission from the individual was balanced (Fig. 4G and H). However, their luminescence efficiencies have discounted to some extent based on this approach (Table S3, ESI†). Moreover, the CIE coordinates of these films were recorded as (0.33, 0.33), which matched well with the standard of pure white light proposed by the International Commission on illumination

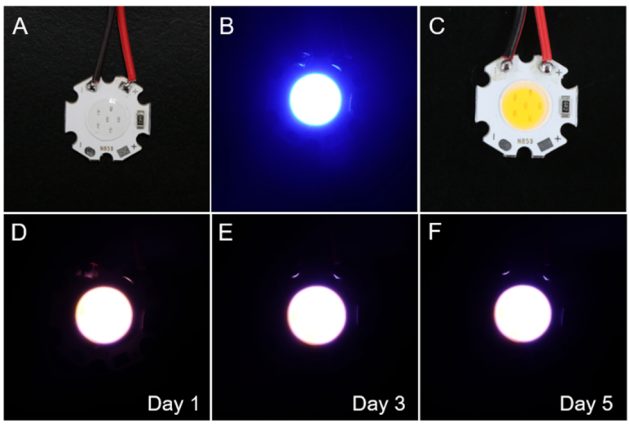

Fig. 5 (A)–(C) Fabrication of while light-emitting device based on blue LEDs by coating a TPP-C2(R)/Dye-O film. (D)–(F) Exhibition of white light emission by the device in 5 days.

(Fig. 4F and I). TPP-C6(R) and TPP-C6(S) also played a similar role in generating white light (Fig. S21, ESI†). All these indicated that the high-quality white light emission can be realized readily with our dyes as hosts. Finally, to demonstrate the potential applications, the white light PMMA film containing TPP-C2(R) and Dye-O was coated on a blue LED (Fig. 5A–C). It was clear that the strong white light can be generated with the LED as an excitation source (Fig. 5D–F). Moreover, as reflected by the fluorescence spectra, less changes in colour and emission intensities can be found during 5 days, indicating a good stability in the use (Fig. S22, ESI†). Thus, it was promising to fabricate it as a device for potential illuminations.

Conclusions

In this work, we have fabricated TPP-based chiral deep-blue dyes by a combination of TPP and binaphthyl units connected by acetylenic bonds. Such a concept can not only endow the molecules with the AEE effect decided by the TPP unit but also remarkably strengthen the molecular conjugation to improve the light absorption ability and luminescence efficiency. This was reflected by ε of more than 8×10^4 cm^{-1} L mol^{-1} in the solutions and Φ_F of $\sim$72% in the PMMA films, which can lead to high brightness of more than 5.5×10^4 cm^{-1} L mol^{-1}. Moreover, the CIE coordinates of these films were (0.15, 0.05), indicating good deep-blue materials for potential applications. The incorporated binaphthyl units can also serve as chiral sources to endow the deep-blue dyes with axial chirality, which was confirmed by the CD spectra. The length of the appended alkoxy chains has an evident effect on self-assemble behaviour, and a longer side chain may induce the formation of definite helical fibers with an opposite direction in the chiral enantiomers, as monitored by SEM and fluorescence microscopy. However, increasing the length of side groups may lead to conversion from AEE to ACQ, as affected by the aggregate-state behaviour caused by such a factor. Moreover, these dyes can be utilized as energy donors to excite other emissions. With their rational mixture with other fluorescent dyes in the PMMA matrix, almost all the energies can be transferred from the donors to the acceptors while a magnified emission can be realized in the acceptors. We also found that the pure white light emission with a CIE coordinate of (0.33, 0.33) can be readily obtained by controllable energy transfer from the donors to the acceptors with PL quantum yields of films approaching 100%. Finally, after coating the films onto the blue LED, the while light-emitting device was fabricated, which showed distinct emissions and good stability. All these indicated that they hold great promise in the optoelectronic application.

Author contributions

M. C. conceived and designed the experiment, and write the paper. X. H. and Y. H. synthesized and characterized the materials. X. H. and C. Z. carried out the fluorescence spectra, SEM and fluorescence microscope tests, *etc.* X. D. conducted the theoretical calculation. C. Q. and H. T. F. carried out the transient PL spectra and absolute quantum yield test. M. M. and B. Z. T. provided suggestions in the study and manuscript. All authors approved the final version of the manuscript.

Conflicts of interest

There are no conflicts to declare.

Acknowledgements

This work is partially supported by the National Natural Science Foundation of China (22275072), the Project of Science and Technology of Guangzhou (2024A04J3712), Shenzhen Key Laboratory of Functional Aggregate Materials (ZDSYS20211021111400001), the Science Technology Innovation Commission of Shenzhen Municipality (KQTD20210811090142053 and JCYJ20220818103007014), Research Foundation of Education Department of Shaanxi Province (20JS005) and Scientific and Technological Innovation Team of Shaanxi Province (2022TD-36).

Notes and references

1 (*a*) X.-H. Zhu, J. Peng, Y. Cao and J. Toncali, *Chem. Soc. Rev.*, 2011, **40**, 3509–3524; (*b*) J. Song, H. Lee, E. G. Jeong, K. C. Choi and S. Yoo, *Adv. Mater.*, 2020, **32**, 1907539; (*c*) G. M. Farinola and R. Ragni, *Chem. Soc. Rev.*, 2011, **40**, 3467–3482; (*d*) S. Ma, S. Du, G. Pan, S. Dai, B. Xu and W. Tuan, *Aggregate*, 2021, **2**, e96; (*e*) Y. Liu, C. Li, Z. Ren, S. Yan and M. R. Bryce, *Nat. Rev. Mater.*, 2018, **3**, 18020.
2 (*a*) E. A. Chandross and C. J. Dempster, *J. Am. Chem. Soc.*, 1970, **92**, 3586–3593; (*b*) J. M. G. Martinho, *J. Phys. Chem.*, 1989, **93**, 6687–6692; (*c*) K. Stavrou, A. Danos, T. Hama, T. Hatakeyama and A. Monkman, *ACS Appl. Mater. Interfaces*, 2021, **13**, 8643–8655; (*d*) B. R. Crenshaw and C. Weder, *Adv. Mater.*, 2005, **17**, 1471–1476.
3 (*a*) J. Mei, N. L. C. Leung, R. T. K. Kwok, J. W. Y. Lam and B. Z. Tang, *Chem. Rev.*, 2015, **115**, 11718–11940; (*b*) J. Yang,

M. Fang and Z. Li, *Aggregate*, 2020, **1**, 6–18; (*c*) M. Fang, J. Yang and Z. Li, *Prog. Mater. Sci.*, 2022, **125**, 100914; (*d*) G. R. Suman, M. Pandey and A. S. J. Chakravarthy, *Mater. Chem. Front.*, 2021, **5**, 1541–1584; (*e*) Y. Song, G. Pan, C. Zhang, C. Wang, B. Xu and W. Tian, *Mater. Chem. Front.*, 2023, **7**, 5104–5119; (*f*) N. Jiang, D. Zhu, Z. Su and M. R. Bryce, *Mater. Chem. Front.*, 2021, **5**, 60–75.

4 (*a*) J. Li, M. Zhao, J. Huang, P. Liu, X. Luo, Y. Zhang, C. Yan, W.-H. Zhu and Z. Guo, *Coordin. Chem. Rev.*, 2022, **473**, 214813; (*b*) F. Zhang, H. Xie, B. Guo, C. Zhu and J. Xu, *Polym. Chem.*, 2022, **13**, 8–13; (*c*) Z. Yang, Z. Mao, Z. Xie, Y. Zhang, S. Liu, J. Zhao, J. Xu, Z. Chi and M. P. Aldred, *Chem. Soc. Rev.*, 2017, **46**, 915–1016; (*d*) Q. Li, Y. Li, T. Min, J. Gong, L. Du, D. L. Phillips, J. Liu, J. W. Y. Lam, H. H. Y. Sung, I. D. Williams, R. T. K. Kwok, C. L. Ho, K. Li, J. Wang and B. Z. Tang, *Angew. Chem., Int. Ed.*, 2020, **132**, 9557–9564; (*e*) M. Chen, Z. Zhang, R. Lin, J. Liu, M. Xie, X. He, C. Zheng, M. Kang, X. Li, H.-T. Feng, J. W. Y. Lam, D. Wang and B. Z. Tang, *Chem. Sci.*, 2024, DOI: **10.1039/D3SC06886B**; (*f*) T. Zang, Y. Xie, S. Su, F. Liu, Q. Chen, J. Jing, R. Zhang, G. Niu and X. Zhang, *Angew. Chem. Int. Ed.*, 2020, **132**, 10089–10093; (*g*) X. Tian, H. Wang, S. Cao, Y. Liu, F. Meng, X. Zheng and G. Niu, *J. Mater. Chem. C*, 2023, **11**, 5987–5994.

5 (*a*) X. Cai and B. Liu, *Angew. Chem., Int. Ed.*, 2020, **59**, 9868–9886; (*b*) F. Hu, S. Xu and B. Liu, *Adv. Mater.*, 2018, **30**, 1801350; (*c*) D. D. La, S. V. Bhosale, L. A. Jones and S. V. Bhosale, *ACS Appl. Mater. Interfaces*, 2018, **10**, 12189–12216; (*d*) E. Ubba, Y. Tao, Z. Yang, J. Zhao, L. Wang and Z. Chi, *Chem. – Asian J.*, 2018, **13**, 3106–3121; (*e*) F. Rizzo and F. Cucinotta, *Isr. J. Chem.*, 2018, **58**, 888–974; (*f*) Q. Wei, N. Fei, A. Islam, T. Lei, L. Hong, R. Peng, X. Fan, L. Chen, P. Gao and Z. Ge, *Adv. Opt. Mater.*, 2018, **6**, 1800512; (*g*) R. Xu, D. Dang, Z. Wang, Y. Zhou, Y. Xu, Y. Zhao, X. Wang, Z. Yang and L. Meng, *Chem. Sci.*, 2022, **13**, 1270–1280; (*h*) W. Ma, Y. Wang, Y. Xue, M. Wang, C. Lu, W. Guo, Y.-H. Liu, D. Shu, G. Shao, Q. Xu, S. Tu and H. Yan, *Chem. Sci.*, 2024, **15**, 4019–4030.

6 (*a*) Y. Li, Y. Tang, W. Hu, Z. Wang, X. Li, X. Lu, S. Chen, W. Huang and Q. Fan, *Adv. Sci.*, 2023, **10**, 2204695; (*b*) S. Liu, H. Ou, Y. Li, H. Zhang, J. Liu, X. Lu, R. T. K. Kwok, J. W. Y. Lam, D. Ding and B. Z. Tang, *J. Am. Chem. Soc.*, 2020, **142**, 15146–15156.

7 (*a*) K. Terayama, S. Habuchi and T. Michinobu, *J. Polym. Sci.*, 2023, **61**, 2276–2291; (*b*) M. Nakamura, I. Kanetani, M. Gon and K. Tanaka, *Angew. Chem., Int. Ed.*, 2024, DOI: **10.1002/ange.202404178**; (*c*) Y. Gui, K. Chen, Y. Sun, Y. Tan, W. Luo, D. Zhu, Y. Xiong, D. Yan, D. Wang and B. Z. Tang, *Chin. J. Chem.*, 2023, **41**, 1249–1259.

8 (*a*) L. Qian, B. Tong, J. Shen, J. Shi, J. Zhi, Q. Dong, F. Yang, Y. Dong, J. W. Y. Lam, Y. Liu and B. Z. Tang, *J. Phys. Chem. B*, 2009, **113**, 9098–9103; (*b*) C. Zheng, Q. Zang, H. Nie, W. Huang, Z. Zhao, A. Qin, R. Hu and B. Z. Tang, *Mater. Chem. Front.*, 2018, **2**, 180–188; (*c*) Z. Qiu, W. Zhao, M. Cao, Y. Wang, J. W. Y. Lam, Z. Zhang, X. Chen and B. Z. Tang, *Adv. Mater.*, 2018, **2**, 1803924.

9 X. Luo, J. Li, C. Li, L. Heng, Y. Q. Dong, Z. Liu, Z. Bo and B. Z. Tang, *Adv. Mater.*, 2011, **23**, 3261–3265.

10 (*a*) Z. Zhao, C. Chen, W. Wu, F. Wang, L. Du, X. Zhang, Y. Xiong, X. He, Y. Cai, R. T. K. Kwok, J. W. Y. Lam, X. Gao, P. Sun, D. L. Phillips, D. Ding and B. Z. Tang, *Nat. Commun.*, 2019, **10**, 768; (*b*) S. Liu, X. Zhou, H. Zhang, H. Qu, J. W. Y. Lam, Y. Liu, L. Shi, D. Ding and B. Z. Tang, *J. Am. Chem. Soc.*, 2019, **141**, 5359–5368.

11 (*a*) S. Rana, S. R. Nayak, S. Patel and S. Vaidyanathan, *J. Mater. Chem. C*, 2024, **12**, 765–818; (*b*) Z. Zhang, D. Dou, R. Xia, P. Wu, E. Spuling, K. Wang, J. Cao, B. Wei, X. Li, J. Zhang, S. Bräse and Z. Wang, *Sci. Adv.*, 2023, **9**, eadf4060; (*c*) P. Sun, D. Liu, F. Zhu and D. Yan, *Nat. Photonics*, 2023, **17**, 264–272; (*d*) X. Wang, G. Zhao, T. Gao, G. Zhang, H. Chen, T. Zhou, Z. Zhang, W. Tian, W. Jiang and Y. Sun, *J. Mater. Chem. C*, 2024, DOI: **10.1039/D3TC04808J**; (*e*) Z. Feng, Z. Cheng, Z. Su, L. Wan, S. Ge, H. Liu, X. Ma, F. Liu and P. Lu, *Adv. Opt. Mater.*, 2024, DOI: **10.1002/adom.202302839**; (*f*) B. Zhou, Z. Qi, M. Dai, C. Xing and D. Yan, *Angew. Chem., Int. Ed.*, 2023, **135**, e202309913.

12 (*a*) M. Chen, L. Li, H. Nie, J. Tong, L. Yan, B. Xu, J. Z. Sun, W. Tian, Z. Zhao, A. Qin and B. Z. Tang, *Chem. Sci.*, 2015, **6**, 1932–1937; (*b*) M. Chen, A. Qin, J. W. Y. Lam and B. Z. Tang, *Coordin. Chem. Rev.*, 2020, **422**, 213472; (*c*) M. Chen, J. Liu, F. Liu, H. Nie, J. Zeng, G. Lin, A. Qin, M. Tu, Z. Kai, H. H. Y. Sung, I. D. Williams, J. W. Y. Lam and B. Z. Tang, *Adv. Funct. Mater.*, 2019, **29**, 1903834; (*d*) M. Chen, R. Chen, Y. Shi, J. Wang, Y. Cheng, Y. Li, X. Gao, Y. Yan, J. Z. Sun, A. Qin, R. T. K. Kwok, J. W. Y. Lam and B. Z. Tang, *Adv. Funct. Mater.*, 2018, **28**, 1704689; (*e*) P. Meti, F. Mateen, D. Y. Hwang, Y.-E. Lee, S.-K. Hong and Y.-D. Gong, *Dyes Pigm.*, 2022, **202**, 110221; (*f*) X.-D. Ying, J.-X. Chen, D.-Y. Tu, Y.-C. Zhuang, D. Wu and L. Shen, *ACS Appl. Mater. Interfaces*, 2021, **13**, 6421–6429; (*g*) L. Yao, K. Fu and G. Liu, *ACS Appl. Mater. Interfaces*, 2023, **15**, 40817–40827; (*h*) G. Gong, H. Wu, T. Zhang, Z. Wang, X. Li and Y. Xie, *Mater. Chem. Front.*, 2021, **5**, 5012–5023; (*i*) H.-Q. Zheng, L. Zhang, M. Lu, X. Xiao, Y. Yang, Y. Cui and G. Qian, *Research*, 2022, 9869510; (*j*) H. F. Pananilath, C. Govind, T. D. Thadathilanickal and V. Karunakaran, *Phys. Chem. Chem. Phys.*, 2023, **25**, 26575–26587.

13 M. Chen, H. Nie, B. Song, L. Li, J. Z. Sun, A. Qin and B. Z. Tang, *J. Mater. Chem. C*, 2016, **4**, 2901–2908.

14 H.-Q. Yin, X.-Y. Wang and X.-B. Yin, *J. Am. Chem. Soc.*, 2019, **141**, 15166–15172.

15 C. Li, J. Liu, Y. Hong, R. Lin, Z. Liu, M. Chen, J. W. Y. Lam, G.-H. Ning, X. Zheng, A. Qin and B. Z. Tang, *Angew. Chem., Int. Ed.*, 2022, **61**, e202202005.

16 H. Wu, Y. Pan, J. Zeng, L. Du, W. Luo, H. Zhang, K. Xue, P. Chen, D. L. Phillips, Z. Wang, A. Qin and B. Z. Tang, *Adv. Optical Mater.*, 2019, **7**, 1900283.

17 H.-T. Feng, X. Zheng, X. Gu, M. Chen, J. W. Y. Lam, X. Huang and B. Z. Tang, *Chem. Mater.*, 2018, **30**, 1285–1290.

18 H. Rao, Z. Liu, M. Chen, C. Zheng, L. Xu, J. Liu, J. W. Y. Lam, B. Li, X. Yang and B. Z. Tang, *Aggregate*, 2024, **5**, e453.

19 (*a*) M. Tang, J. Wen, Y. Sun, Q. Hou, X. Cai, W. He, X. Xie, H. Ding, F. Li, L. Zheng, Y. Shi and Q. Cao, *Adv. Funct.*

Mater., 2024, DOI: 10.1002/adfm.202314130; (*b*) M. Dong, L. Liao, C. Li, Y. Mu, Y. Huo, Z.-M. Su and F. Liang, *J. Mater. Chem. C*, 2024, **12**, 443–448.

20 (*a*) A. H. Ashoka, I. O. Aparin, A. Reisch and A. S. Klymchenko, *Chem. Soc. Rev.*, 2023, **52**, 4525–4548; (*b*) G. Jiang, H. Liu, H. Liu, G. Ke, T.-B. Ren, B. Xiong, X.-B. Zhang and L. Yuan, *Angew. Chem. Int. Ed.*, 2024, **136**, e202315217.

21 (*a*) Y. Xia, A. Hao and P. Xing, *ACS Nano*, 2023, **17**, 21993–22003; (*b*) J. Kwon, K. H. Park, W. J. Choi, N. A. Kotov and J. Yeom, *Acc. Chem. Res.*, 2023, **56**, 1359–1672; (*c*) S. Huang, H. Yu and Q. Li, *Adv. Sci.*, 2021, **8**, 2002132; (*d*) H. Li, X. Mao, H. Wang, Z. Geng, B. Xiong, L. Zhang, S. Liu, J. Xu and J. Zhu, *Macromolecules*, 2020, **53**, 4214–4223; (*e*) H. Li, E. J. Cornel, Z. Fan and J. Du, *Chem. Sci.*, 2022, **13**, 14179–14190.

22 (*a*) J. Zhang, Q. Liu, W. Wu, J. Peng, H. Zhang, F. Song, B. He, X. Wang, H. H. Y. Sung, M. Chen, B. S. Li, S. H. Liu, J. W. Y. Lam and B. Z. Tang, *ACS Nano*, 2019, **13**, 3618–3628; (*b*) Y. S. Lee, *Self-Assembly and Nanotechnology: a Force Balance Approach*, John Wiley & Sons, 2008.

23 (*a*) M. J. Frisch, *et al. Gaussian 16*, Gaussian, Inc., Wallingford, CT, 2016; (*b*) S. Grimme, S. Ehrlich and L. Goerigk, *J. Comput. Chem.*, 2011, **32**, 1456–1465; (*c*) S. Grimme, J. Antony, S. Ehrlich and H. Krieg, *J. Chem. Phys.*, 2010, **132**, 154104.

24 (*a*) L. Pan, Y. Cai, H. Wu, F. Zhou, A. Qin, Z. Wang and B. Z. Tang, *Mater. Chem. Front.*, 2018, **2**, 1310–1316; (*b*) K. R. J. Thomas, J. T. Lin, M. Velusamy, Y.-T. Tao and C.-H. Chuen, *Adv. Funct. Mater.*, 2004, **14**, 83–90; (*c*) W. Qin, N. Alifu, J. W. Y. Lam, Y. Cui, H. Su, G. Liang, J. Qian and B. Z. Tang, *Adv. Mater.*, 2020, **32**, 2000364.

25 (*a*) Q. Song, S. Goia, J. Yang, S. C. L. Hall, M. Staniforth, V. G. Stavros and S. Perrier, *J. Am. Chem. Soc.*, 2021, **143**, 382–389; (*b*) B. Song, L. Zhang, J. Sun, J. W. Y. Lam and B. Z. Tang, *Angew. Chem., Int. Ed.*, 2023, **62**, e202302543.

26 (*a*) P. Q. Nhien, J.-H. Tien, T. T. K. Cuc, T. M. Khang, N. T. Trung, B. T. B. Hue, J. I. Wu and H.-C. Lin, *J. Mater. Chem. C*, 2022, **10**, 18241–18257; (*b*) N. T. Trung, P. Q. Nhien, T. T. K. Cuc, C.-H. Wu, B. T. B. Hue, J. I. Wu, Y.-K. Li and H.-C. Lin, *ACS Appl. Mater. Interfaces*, 2023, **15**, 15353–15366; (*c*) P. Q. Nhien, T. T. K. Cuc, T. M. Khang, C.-H. Wu, B. Z. B. Hue, J. I. Wu, B. W. Mansel, H.-L. Chen and H.-C. Lin, *ACS Appl. Mater. Interfaces*, 2020, **12**, 47921–47938; (*d*) P. Q. Nhien, H.-K. Chang, T. T. K. Cuc, T. M. Khang, C.-H. Wu, B. T. B. Hue, J. I. Wu and H.-C. Lin, *Sens. Actuators, B*, 2022, **372**, 132634.

27 (*a*) Z. Chen, C.-L. Ho, L. Wang and W.-Y. Wong, *Adv. Mater.*, 2020, **32**, 1903269; (*b*) H. Zhang, Q. Su and S. Chen, *Nat. Commun.*, 2020, **11**, 2826.

28 (*a*) N.-C. Chiu, K. T. Smith and K. C. Stylianou, *Coordin. Chem. Rev.*, 2022, **459**, 214441; (*b*) Y. Huang, E.-L. Hsiang, M.-Y. Deng and S.-T. Wu, *Light: Sci. Appl.*, 2020, **9**, 105; (*c*) B. Kumari, R. Dahiwadkar and S. Kanvah, *Aggregate*, 2022, **3**, e191.